Supporting Information

# Highly atom-economic bioactive nanocarrier for synergistic enhanced antitumor with reduced liver injury

Jiacheng Wang, Wenshu Qiao, Haitian Zhao, Jianjun Cheng, Ying Han, Xin Yang *

School of Chemistry and Chemical Engineering, Harbin Institute of Technology, No.92 West Dazhi Street, Nan Gang District, Harbin, Heilongjiang, 150001, P.R.China

***Corresponding Author:** yangxin@hit.edu.cn

Experimental procedures

Separation, extraction and identification of active natural products.

The following compounds were isolated and purified according to our previous experience accumulation and experimental results of the laboratory[1-3].

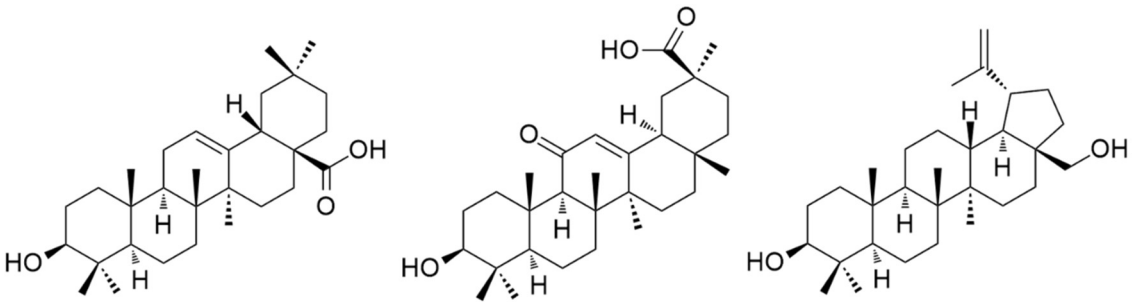


**Oleanolic acid** **Glycyrrhetinic acid** **Betulin**

**Scheme 1.** Structural formula of active natural products

***Oleanolic acid (OA)*** crude extract were obtained by chemical fractionation of 95% (v/v) ethanol extract of *Dry papaya powder*. The crude extracts were eluted with petroleum ether and carbon tetrachloride. The obtained extracts were then separated and purified by macroporous resin (D4020). Then repeated and purification on a reversed-phase C18 column.

***Betulin (Bet)*** crude extracts of *Dry birch bark* were ultrasonically extracted with 95% (v/v) methanol. The crude extracts were eluted with petroleum ether and ethyl acetate. The obtained extract was purified by macroporous resin (D101). Then repeated purification on reverse-phase C18 column.

***Glycyrrhetinic acid (GA)*** was obtained by repeated decoction. The extraction of the licorice powder is made with boiling water. The concentrate is heated under reflux with 5% dilute sulfuric acid, washed to neutral, dried and dissolved in hot chloroform, filtered and subjected to column chromatography. Recrystallization gave glycyrrhetinic acid crystals.

Analysis was conducted by high-performance liquid chromatography (HPLC) and compounds were identified by comparing with standards. Furthermore, completion of the structural characterization was performed by mass spectrometry data and protonic nuclear magnetic resonance spectrometric data and comparison with the previously published data.

Replica-exchange molecular dynamics (REMD) simulation

To understand the self-assembly process, all-atom replica exchange molecular dynamics (REMD) simulations was performed using Gromacs software.[4] Carriers (OA) and drug (PTX) in simulation system, the number is 14 and 1, and the simulation used the Charmm36 force

field, TIP3P model was used to model aqueous solution sodium ions were added to balance the system negative charge. The long-range electrostatic action was calculated by PME method, the cut-off radius was set to 10 nm, and the van der Waals force interaction cut-off radius was 12 nm. The REMD simulation system is divided into two parts, OP and UP. The two systems are first subjected to a 200 ps MVT balance at 300K. In the temperature range of 300K~700K, the online server (http://folding mc uu se/remd/) was used to predict the temperature distribution of each copy, and 35 copies were generated.[5] All replicas were run in parallel, each replica was subjected to a 50 ns REMD simulation, the simulated time step was set to 2fs, and replica exchange attempts between adjacent replicas were made every 500 steps. The trajectory was saved every 10 ps, and the simulation process was visually analyzed using YASARA and VMD software. All the above calculations are conducted on the MolDesigner Molecular Simulation Platform[6, 7].

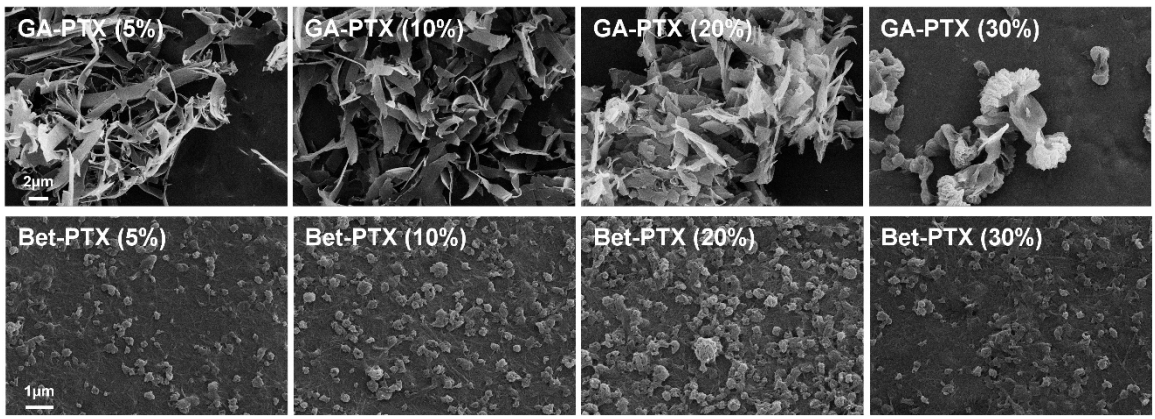


**Figure S1 SEM images of GA-PTX NPs and Bet-PTX NPs.** All GA-PTX NPs are nanosheets morphology and all Bet-PTX NPs are nanofibers morphology

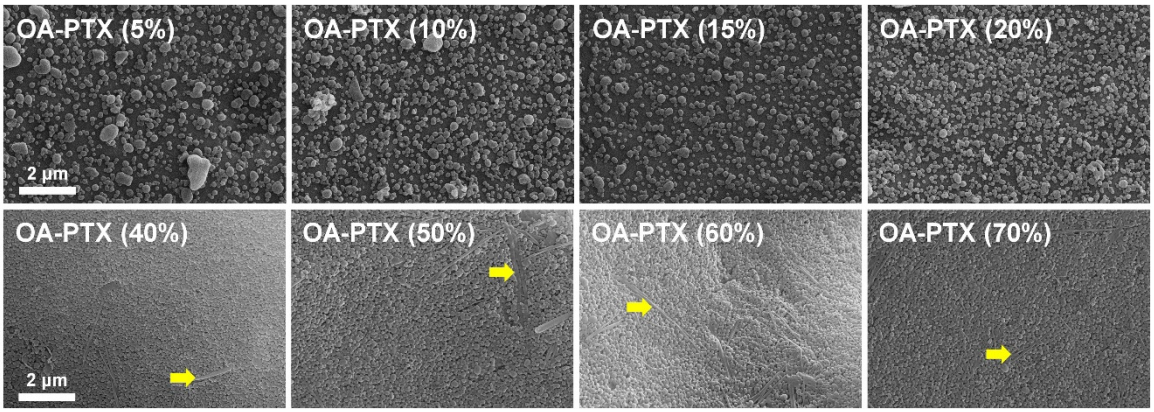


**Figure S2 SEM images of OA-PTX NPs.** The nanofibers morphology is obvious at the yellow arrow.

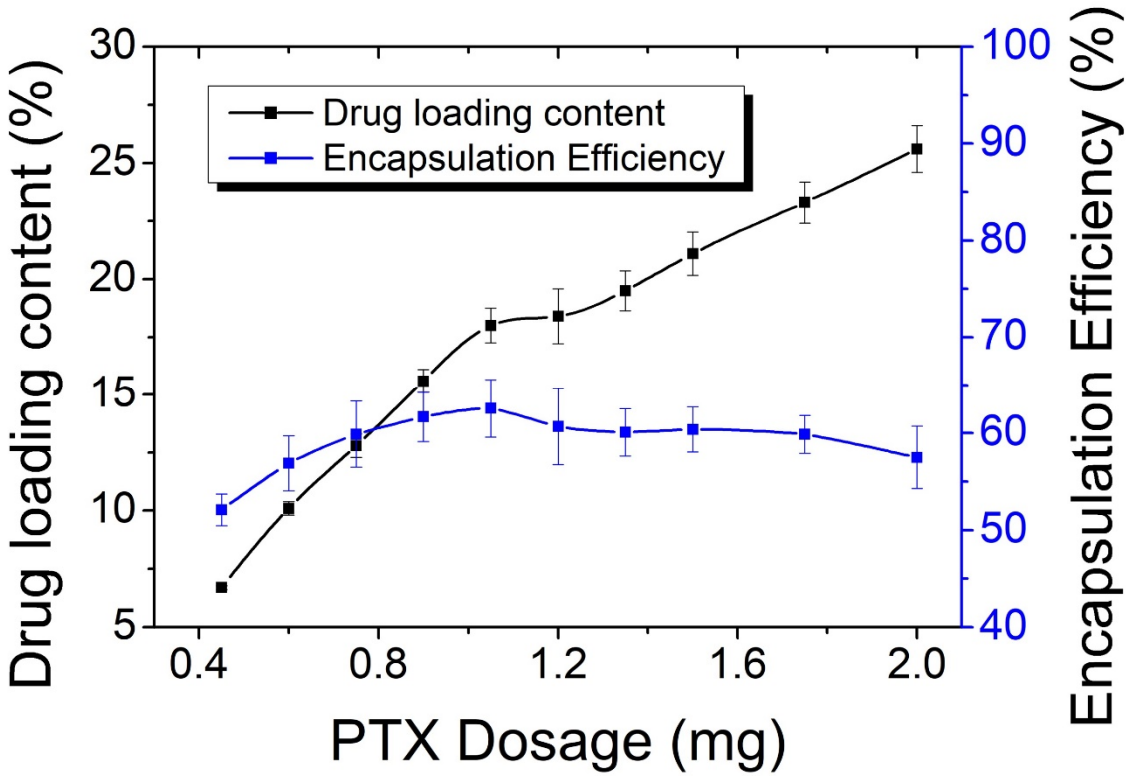


**Figure S3 Drug loading and entrapment efficiency of OA-PTX.** Optimal drug loading and encapsulation efficiency of OA-PTX NPs are 17.1% and 62.6%, respectively**.**

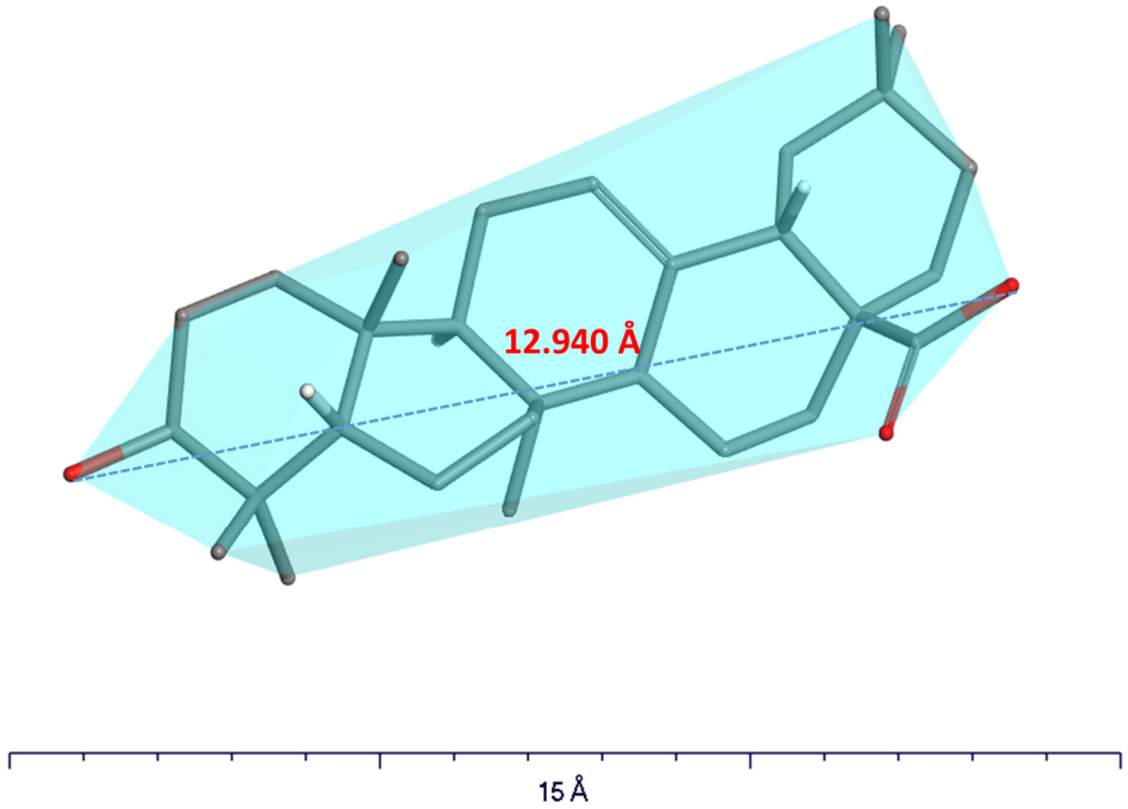


**Figure S4. The molecular length of OA (12.940 Å) as measured by Materials Studio 8.0.**

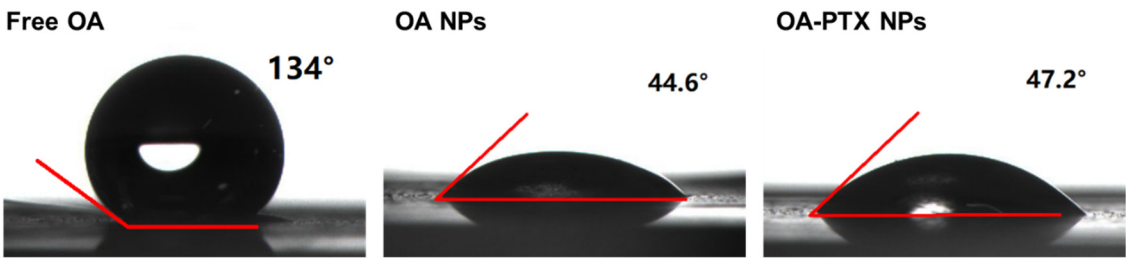


**Figure S5. Wettability measurement of NPs.** Three-phase contact angles of free OA and OA NPs and OA-PTX NPs. All NPs prepared by the emulsion solvent evaporation method showed substantially improved hydrophilicity.

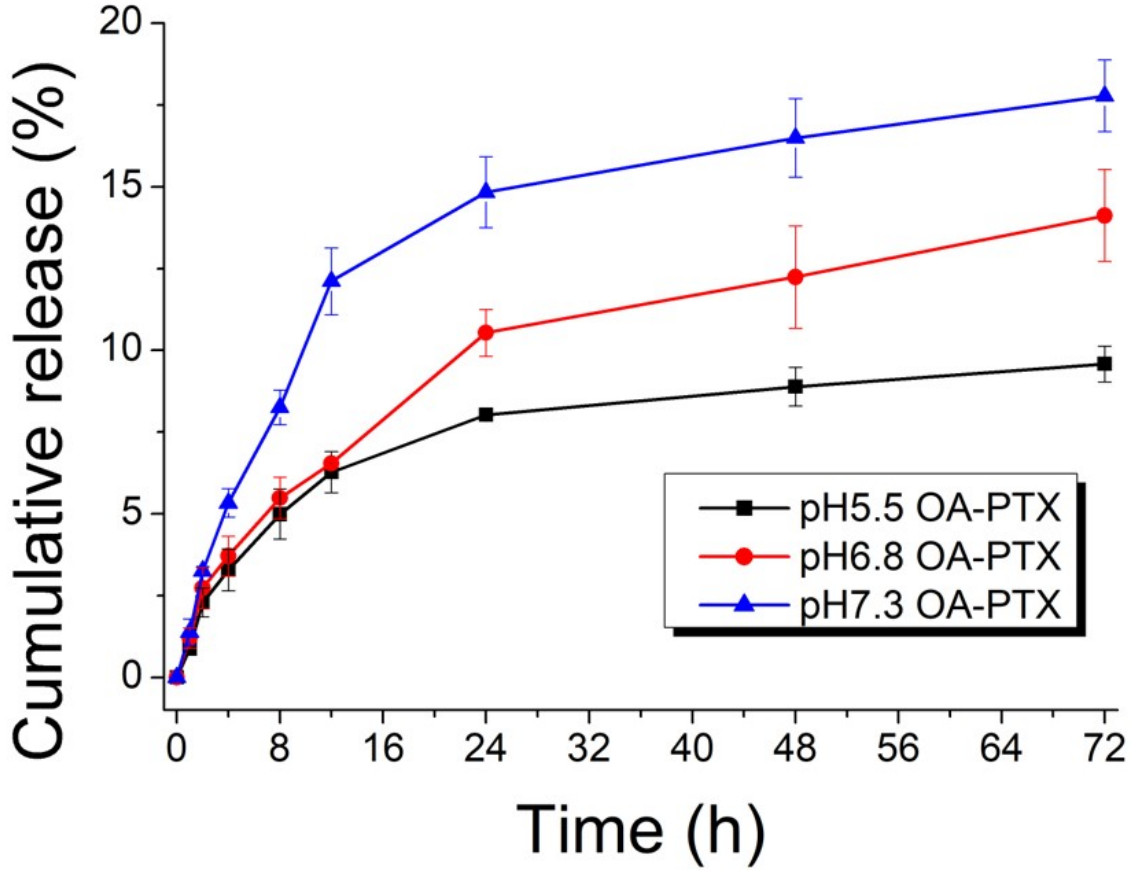


**Figure S6. OA-PTX NPs drug release profile.** Drug release profiles of OA-PTX NPs at three different pH values (7.3, 6.8, and 5.5) at room temperature. Data are expressed as mean ± s.e.m. (n = 3)

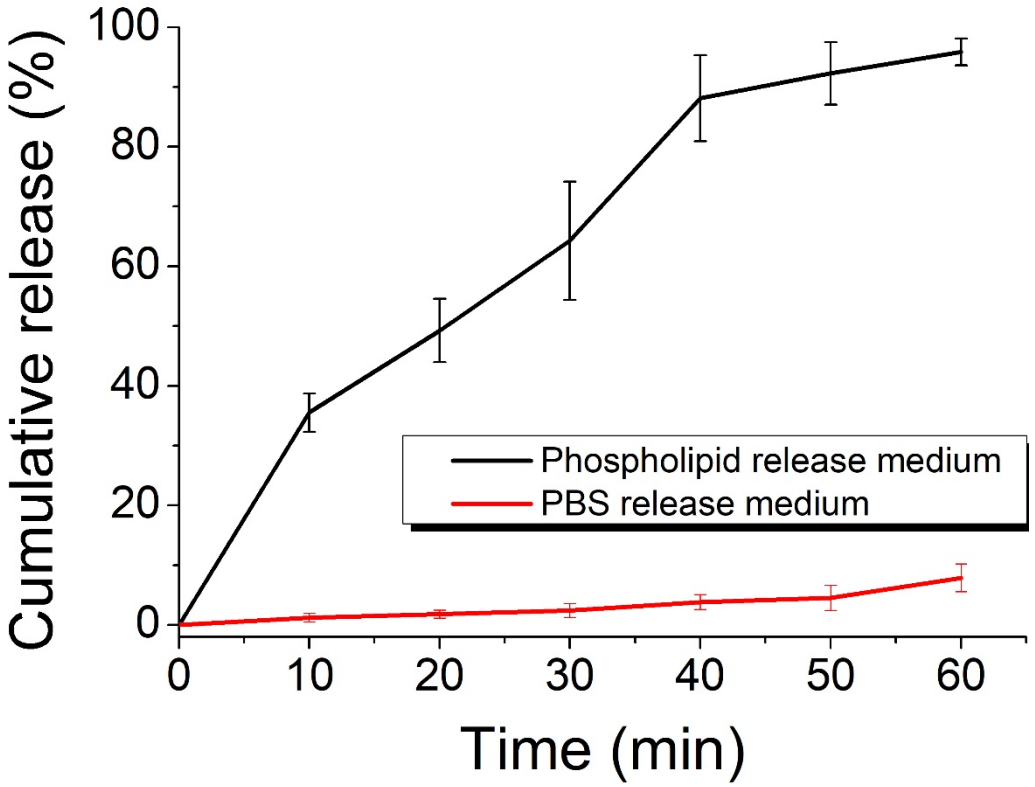


**Figure S7.** Drug release in PBS medium containing 20% lecithin. Data are expressed as mean ± s.e.m. (n = 3)

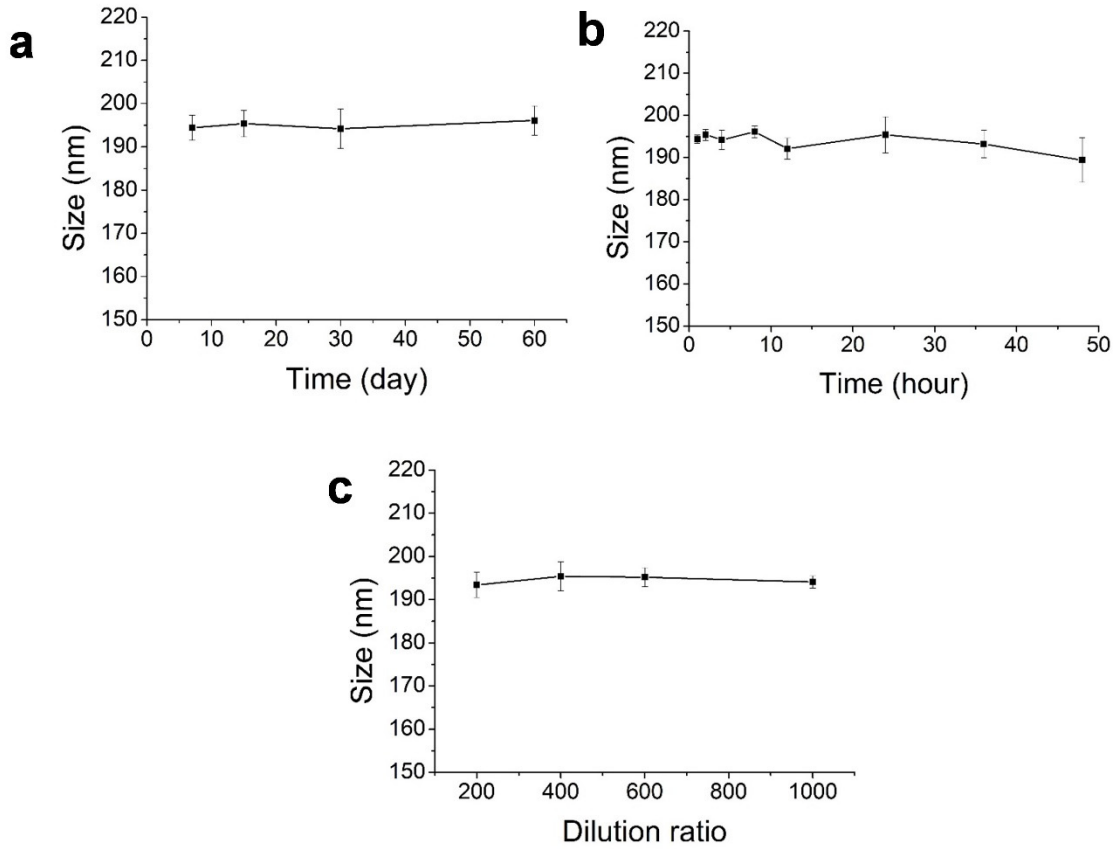


**Figure S8. Stability of OA-PTX NPs. a**. OA-PTX NPs of freeze-dried powders were redispersion in double-distilled water at different storage times. **b**. Stability in the presence of serum **c**. OA-PTX NPs size after different dilution factors

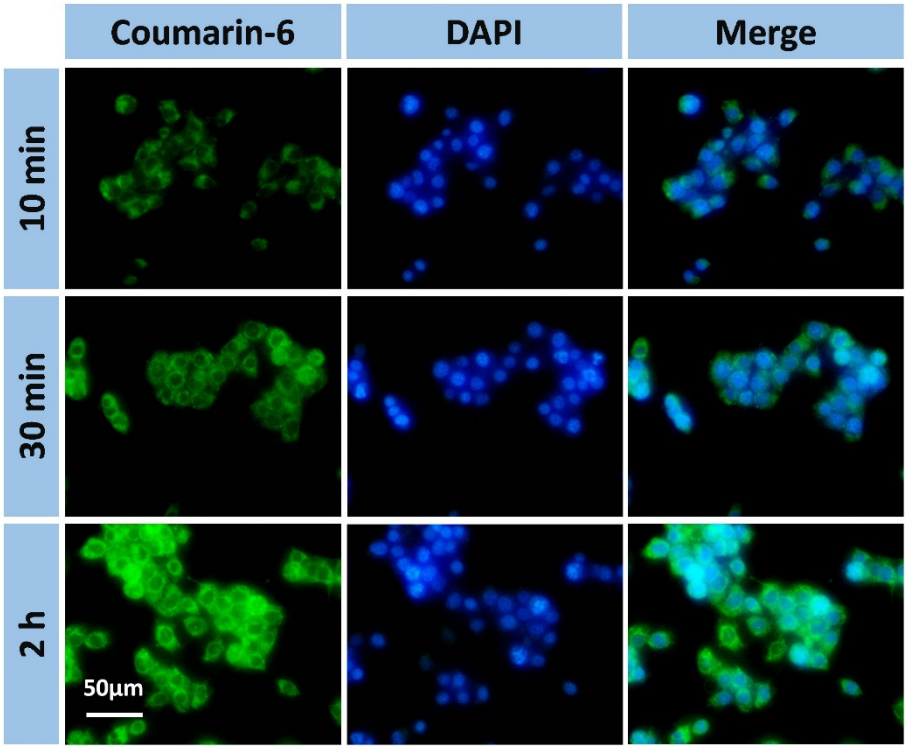


**Figure S9. Cell uptake representative microimages.** 4T1 cells incubated with OA-PTX NPs at different times. Magnification ×400

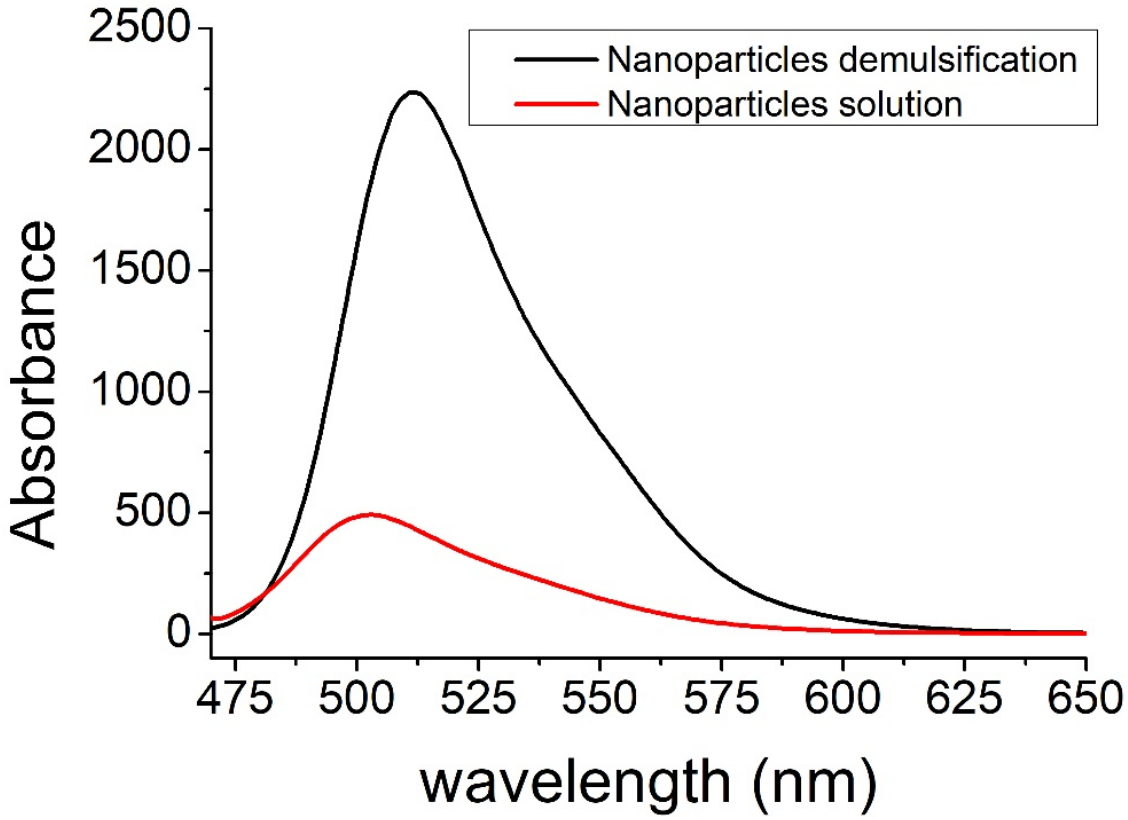


**Figure S10. Fluorescence intensity of fluorescently labeled nanoparticles before and after demulsification.**

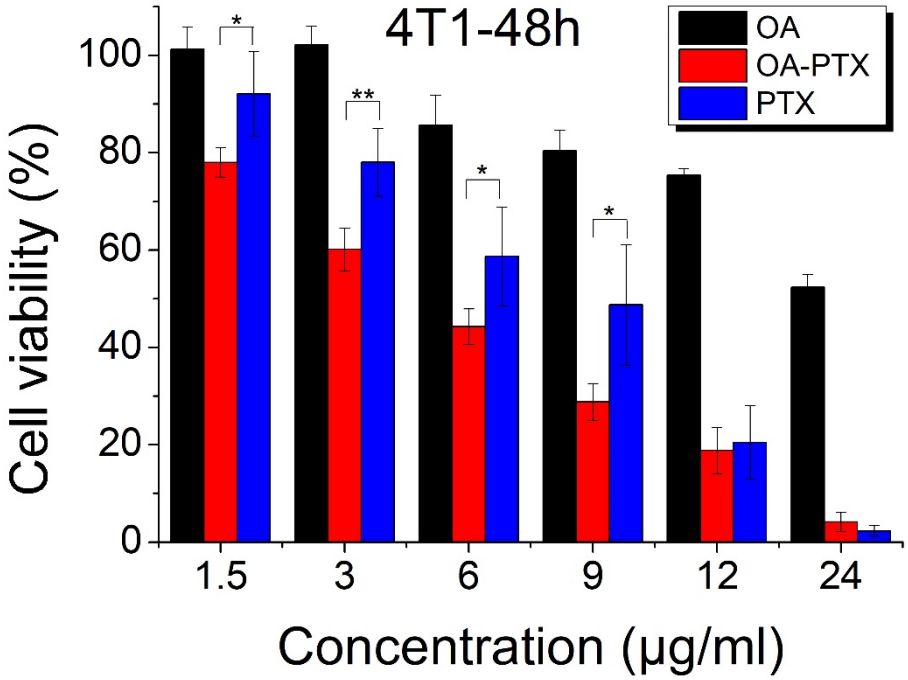


**Figure S11. The growth inhibitory effects of OA-PTX NPs on 4T1 cells for 48h. (*P < 0.05, **P < 0.01)**

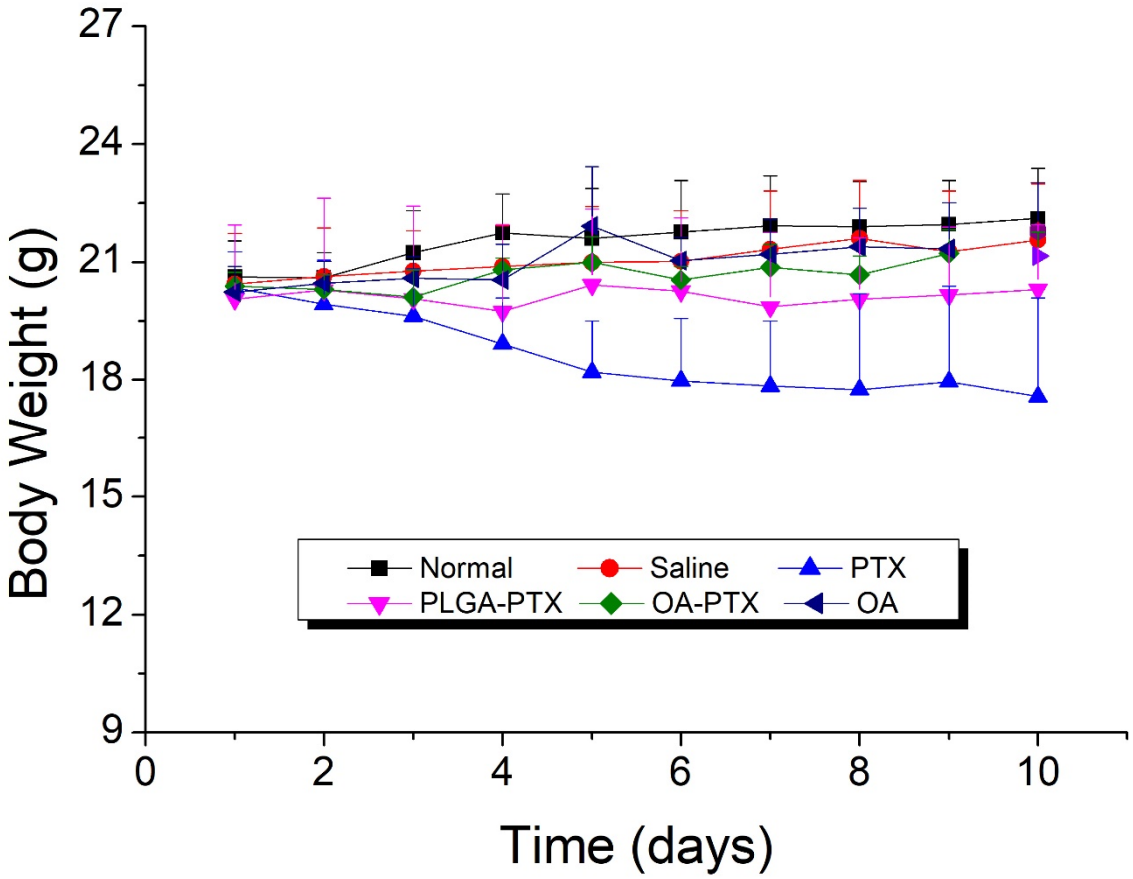


**Figure S12. Body weight change of mice after different nano-formulations treatment.**

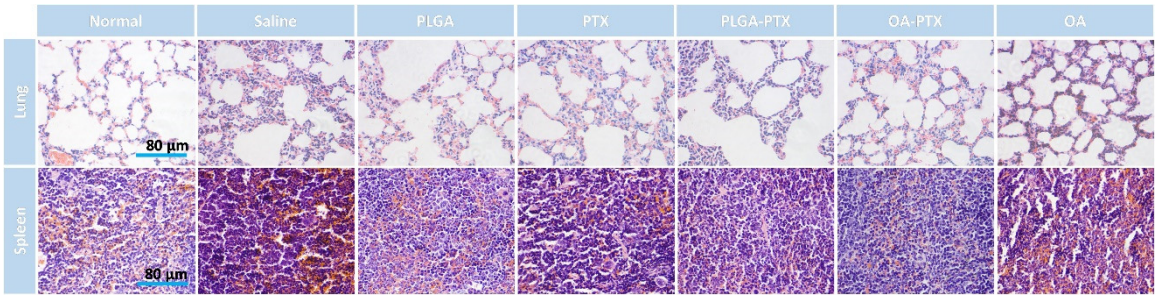


**Figure S13. Supplementary data for Haematoxylin and eosin (H&E).**

**Table S1. Characterization of OA-PTX NPs by DLS.**

| Formula abbreviation | Particle Diameter (nm) | PDI | Zeta Potential (mV) |
|---|---|---|---|
| OA-PTX (5%) | 281±3 | 0.05±0.02 | -20.2±1.6 |
| OA-PTX (10%) | 271±5 | 0.04±0.01 | -20.0±1.6 |
| OA-PTX (15%) | 263±7 | 0.05±0.03 | -19.7±1.5 |
| OA-PTX (20%) | 252±6 | 0.04±0.02 | -15.2±1.2 |
| OA-PTX (25%) | 283±8 | 0.1±0.03 | -12.1±0.9 |
| OA-PTX (30%) | 365±10 | 0.24±0.09 | -9.2±0.7 |
| Data are presented as mean ± s.d. (*n = 3*) | | | |

**Table S2. Characterization of OA-PTX NPs by DLS.**

| Formula abbreviation | Particle Diameter (nm) | PDI | Zeta Potential (mV) |
|---|---|---|---|
| GA-PTX (5%) | 3001±1596 | 1 | -17.2±1.3 |
| GA-PTX (10%) | 2632±956 | 1 | -21.3±1.7 |
| GA-PTX (15%) | 3231±1326 | 1 | -15.9±1.2 |
| GA-PTX (20%) | 3585±1548 | 1 | -15.7±1.2 |
| GA-PTX (25%) | 3130±2036 | 1 | -16.2±1.2 |
| GA-PTX (30%) | 4702±1986 | 1 | -12.5±1.0 |
| Data are presented as mean ± s.d. (*n = 3*) | | | |

**Table S3. Characterization of OA-PTX NPs by DLS.**

| Formula abbreviation | Particle Diameter (nm) | PDI | Zeta Potential (mV) |
|---|---|---|---|
| Bet-PTX (5%) | 681±68 | 0.45±0.15 | -8.5±0.7 |
| Bet-PTX (10%) | 730±59 | 0.50±0.14 | -6.6±0.5 |
| Bet-PTX (15%) | 683±32 | 0.57±0.16 | -10.7±0.8 |
| Bet-PTX (20%) | 913±67 | 0.67±0.13 | -7.6±0.6 |
| Bet-PTX (25%) | 736±82 | 0.52±0.18 | -9.4±0.7 |
| Bet-PTX (30%) | 679±55 | 0.67±0.20 | -6.1±0.5 |
| Data are presented as mean ± s.d. (*n = 3*) | | | |

**Table S4. Fluorescence intensity of tumor tissue at different time.**

| Tumor tissue | | | | | | |
|---|---|---|---|---|---|---|
| Time (h) | 1 | 2 | 4 | 8 | 12 | 24 |
| Average fluorescence intensity | 18616 | 16254 | 13887 | 10212 | 6652 | 2602 |

**Table S5. The fluorescence intensity of main tissues at different time.**

| Time (h) | Main tissues | | | | | |
|---|---|---|---|---|---|---|
| | Heart | Liver | Spleen | Lung | Kidney | Tumor |
| 1 | 556 | 3732 | 993 | 1366 | 3849 | 3098 |
| 8 | 216 | 961 | 455 | 817 | 2178 | 2312 |
| 24 | 105 | 468 | 254 | 262 | 761 | 659 |

# References


1. K. Zhi, H. Zhao, X. Yang, H. Zhang, J. Wang, J. Wang and J. M. Regenstein, *Nanoscale*, 2018, **10**, 3639-3643.
2. K. Zhi, H. Zhao, X. Yang, H. Zhang, J. Wang and Z. Wang, *ChemPlusChem*, 2018, **83**, 797-803.
3. J. Wang, H. Zhao, K. Zhi and X. Yang, *ACS Applied Materials & Interfaces*, 2020, **12**, 6827-6839.
4. B. Hess, C. Kutzner, D. v. d. Spoel and E. Lindahl, *J. Chem. Theory Comput.*, 2008, **4**, 435-447.
5. A. Patriksson and D. v. d. Spoel, *Physical chemistry chemical physics : PCCP*, 2008, **10**, 2073-2077.
6. E. Krieger, T. Darden, S. B. Nabuurs and A. V. Finkelstein, *Proteins Structure Function & Bioinformatics*, 2004, **57**, 678-683.
7. W. Humphrey, A. Dalke and K. Schulten, *J. Mol. Graphics*, 1996, **14**, 33-38.